THE JOURNAL OF PHYSICAL CHEMISTRY Letters

Letter

pubs.acs.org/JPCL

Density, Elasticity, and Stability Anomalies of Water Molecules with Fewer than Four Neighbors

Chang Q Sun,*[,†,‡] Xi Zhang,[‡,§] Ji Zhou,[∥] Yongli Huang,[†] Yichun Zhou,[†] and Weitao Zheng*[,⊥]

[†]Key Laboratory of Low-Dimensional Materials and Application Technologies and Faculty of Materials and Optoelectronics and Physics, Xiangtan University, Hunan 411105, China

[‡]School of Electrical and Electronic Engineering, Nanyang Technological University, Singapore 639798

[§]Center for Coordination Bond Engineering, College of Materials Science and Engineering, China Jiliang University, Hangzhou 310018, China

[∥]State Key Laboratory of New Ceramics and Fine Processing, Department of Materials Science and Engineering, Tsinghua University, Beijing 100084, China

[⊥]School of Materials Science, Jilin University, Changchun 130012, China

Supporting Information

ABSTRACT: Goldschmidt−Pauling contraction of the H−O polar-covalent bond elongates and polarizes the other noncovalent part of the hydrogen bond (O:H−O), that is, the O:H van der Waals bond, significantly, through the Coulomb repulsion between the electron pairs of adjacent oxygen (O−O). This process enlarges and stiffens those H_2O molecules having fewer than four neighbors such as molecular clusters, hydration shells, and the surface skin of water in liquid state. The shortening of the H−O bond raises the local density of bonding electrons, which in turn polarizes the lone pairs of electrons on oxygen. The stiffening of the shortened H−O bond increases the magnitude of the O1s binding energy shift, causes the blue shift of the H−O phonon frequencies, and elevates the melting point of molecular clusters and ultrathin films of water, which gives rise to their elastic, hydrophobic, ice-like, and low-density behavior at room temperature.

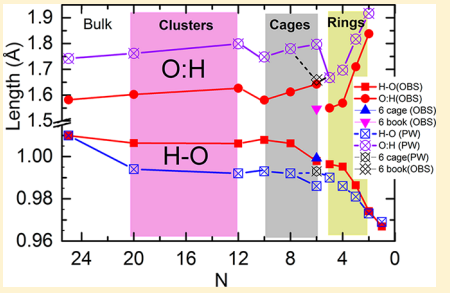

SECTION: Physical Processes in Nanomaterials and Nanostructures

Under-coordinated water molecules refer to those with fewer than the ideal four neighbors as in the bulk of water.[1−4] They occur in terminated hydrogen-bonded networks in the skin of a large volume of water and in the gaseous state. It would be appropriate to call the surface as the skin shells or surface skin because of the volumetric nature. Such under-coordinated water molecules exhibit even more fascinating behavior than those fully coordinated ones.[4−12] For example, water droplets encapsulated in hydrophobic nanopores[13,14] and ultrathin water films on graphite, silica, and selected metals[7,15−20] behave like ice at room temperature; that is, they melt at a temperature higher than the melting point of water in bulk (monolayer ice melts at 325K).[21] (Empirically, the melting point is the temperature at which the vibration amplitude of an atom is increased abruptly to >3% of its diameter irrespective of cluster size.)[22,23] More interestingly, the monolayer film of water is hydrophobic.[20,24]

Molecular under-coordination enlarges the O1s core-level shift and causes a blue shift of the H−O phonon frequency (ω_H) of bulk water. The O1s level energy is 536.6 eV in the bulk of water,[25] 538.1 eV in the surface of water, and 539.8 eV in gaseous molecules.[26] The ω_H phonon frequency has a peak centered at 3200 cm^{-1} for the bulk, 3475 and 3450 cm^{-1} for the surfaces of water and ice,[27] and 3650 cm^{-1} for gaseous molecules.[28−30] Such abnormal behaviors of electronic binding energy and phonon stiffness of under-coordinated water molecules are associated with a 5.9% expansion of the surface O−O distance at room temperature.[5,31−34] In addition, the volume of water molecules confined to 5.1 and 2.8 nm TiO_2 pores increases by 4 and 7.5%, respectively, with respect to that in bulk.[35]

Achieving a consistent understanding of these anomalies caused by molecular under-coordination remains a great challenge. We meet this challenge with a union of Goldschmidt and Pauling's (GP) "under-coordination-induced atomic radius contraction",[36−38] Anderson's "strong localization",[39] and our "O:H−O hydrogen bond" approach.[40] On the basis of this framework, we show that under-coordination-induced GP H−O bond contraction and the interelectron-pair Coulomb repulsion dictate the observed attributes of the enlarged O1*s* core-level and Raman frequency shifts, volume expansion, charge entrapment and polarization,[41] as well as the "ice-like and hydrophobicity" nature of such water molecules at room temperature.

Received: May 18, 2013
Accepted: July 3, 2013

   dx.doi.org/10.1021/jz401029z | J. Phys. Chem. Lett. XXXX, XXX, XXX−XXX

Figure 1 illustrates the basic structural unit of the segmented "$O^{\delta-}$:$H^{\delta+}$−$O^{\delta-}$" hydrogen bond (O:H−O will be used for simplicity) in hydrogen-bonded networks.[40,42] The ":" represents the electron lone pair of the sp^3-hybridized oxygen. δ is a fraction that denotes the polarity of the H−O polar-covalent bond and is determined by the difference in electronegativity of O and H. The hydrogen bond comprises both the O:H van der Waals (vdW) bond and the H−O polar-covalent bond, as opposed to either of them alone. The H−O bond is much shorter, stronger, and stiffer (0.1 nm, 4.0 eV, 3000 cm^{-1}) than the O:H bond (0.2 nm, 0.1 eV, 200 cm^{-1}).[42] The bond energy characterizes the bond strength, while the vibration frequency characterizes the bond stiffness. In addition to the short-range interactions within the O:H and the H−O segments, Coulomb repulsion between the bonding electron pair "-" and the nonbonding electron lone pair ":" (the pair of dots on O in Figure 1) is of vital importance to the relaxation of the O:H−O bond-angle−length−stiffness under external stimulus.[40,42]

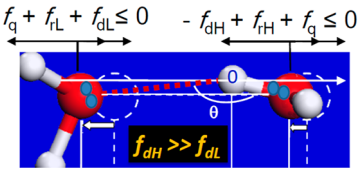

Figure 1. Forces of interelectron-pair (pairing dots) Coulomb repulsion f_q, resistance of deformation f_{rx}, and under-coordination-induced bond contraction f_{dx} as well as the direction and degree of displacement for each O atom (in red) with respect to the H atom as the coordination origin. Subscripts L and H represent the O:H and the H−O segments of the O:H−O hydrogen bond, respectively.

In combination with the forces of Coulomb repulsion (f_q) and resistance to deformation (f_{rx}), each of the forces f_{dx} (x = L represents the O:H and x = H the H−O bond) can drive the hydrogen bond to relax. The two oxygen atoms involved in the O:H−O bond will move in the same direction simultaneously but by different amounts with respect to the H atom that serves as the point of reference (Figure.1).

According to Goldschmidt[37] and Pauling,[36] the radius of an atom shrinks once its coordination number (CN) is reduced. If the atomic CN is reduced relative to the standard of 12 in the bulk (for an fcc structure) to 8, 6, 4, and 2, the radius will contract by 3, 4, 12, and 30%, respectively.[37,38] Furthermore, the bond contraction will be associated with a deepening of the interatomic potential well or an increase of the bond energy,[43] according to the general rule of energy minimization during the spontaneous process of relaxation. In other words, bonds between under-coordinated atoms become shorter and stronger. Such a bond-order−length−strength (BOLS) correlation is formulated as follows (illustrated in Supporting Information):[43]

$$\begin{cases} C_z = d_z/d_b = 2\{1 + \exp[(12 - z)/(8z)]\}^{-1} & \text{(bond - contraction - coefficient)} \\ C_z^{-m} = E_z/E_b & \text{(bond - strengthening - coefficient)} \end{cases} \quad (1)$$

where m (= 4 for water[44]) relates the bond energy E_z changes to the bond length d_z. The subscript z denotes the number of neighbors that an atom has, and b denotes an atom in the bulk.

Bond order (CN) loss causes a localization of electrons, according to Anderson.[39] The bond contraction raises the local density of electrons in the core bands and electrons shared in the bonds. The electron binding energy in the core band will shift accordingly as the potential well deepens (called entrapment, T). The densification and entrapment of the core and bonding electrons in turn polarize the nonbonding electrons (lone pair in this case), raising their energy closer to E_F.[45]

However, molecular clusters, surface skins, and ultrathin films of water may not follow the BOLS precisely. One water molecule interacts with its neighbors through the hydrogen bond that is segmented into the nonbonding lone pair (van der Waals bond) and the covalent bond. The involvement of the weak lone pair interaction and the interelectron−pair repulsion prevent the two segments of the hydrogen bond from following the BOLS mechanism simultaneously. The binding energy difference between the O:H and H−O and the presence of the interelectron-pair repulsion define the H−O covalent bond to be the "master" that contracts to a smaller degree than which eq 1 predicts. The contraction of the H−O bond lengthens and softens the 'slave' O:H bond by repulsion. In other usual materials, all bonds contract by the same extent simultaneously.

Because of the difference in stiffness between the O:H and the H−O segments,[40] the softer O:H segment always relaxes more in length than the stiffer H−O covalent bond does: $|\Delta d_L| > |\Delta d_H|$. Meanwhile, the repulsion polarizes the electron pairs during relaxation, which increases the viscosity of water.

The relatively weaker O:H interaction contributes insignificantly to the Hamiltonian and its related properties, such as the core-level shift. However, the O:H bond-length−stiffness relaxation determines the vibration frequency of the O:H phonons (ω_L< 300 cm^{-1}) and the energy for freezing a water molecule from a liquid state.

The stiffening of the H−O bond increases the O1s core level shift, ΔE_{1s}, elevates the critical temperature, T_C, for phase transition (superheating), and increases the H−O phonons frequency ω_H according to the following relations:[46−48]

$$\left.\begin{matrix} T_C \\ \Delta E_{1s} \\ \Delta\omega_x \end{matrix}\right\} \propto \begin{cases} E_H \\ E_H \\ \sqrt{E_x}/d_x = \sqrt{Y_x}d_x \end{cases} \quad (2)$$

E_x is the cohesive energy of the respective bond (x = L or H). Theoretical reproduction of the critical temperature T_C for ice VII−VIII phase transition under compression confirmed that the H−O bond energy determines the T_C.[40] The shift of the O1s core level energy from that of an isolated oxygen atom is also proportional to the H−O bond energy.[46] Finally, the phonon frequency shift is proportional to the square root of the bond stiffness, which is the product of the Young's modulus ($Y_x \propto E_x d_x^{-3}$) and the bond length.[40,42]

The slight shortening of the H−O covalent bond and the significant lengthening of the O:H interaction result in the O:H−O bond lengthening and molecular volume expansion.

dx.doi.org/10.1021/jz401029z | J. Phys. Chem. Lett. XXXX, XXX, XXX−XXX

Further polarization and an increase in the elasticity and viscosity of the molecules will occur. For a molecular cluster of a given size, the BOLS effect becomes more significant as one moves away from the center. The smaller the molecular cluster, the stronger the BOLS effect will be because of the higher fraction of under-coordinated molecules. Therefore, we expect that molecular clusters, ultrathin films, and the skin of the bulk of water could form an ice-like, low-density phase that is stiffer, hydrophobic, and more thermally stable compared with the bulk liquid.

To verify our hypotheses and predictions as discussed above, we calculated the angle−length−stiffness relaxation dynamics of the O:H−O bond and the total binding energy of water clusters as a function of the number of molecules N. Structural optimizations of $(H_2O)_N$ clusters were performed by Dmol^3 code using Perdew and Wang's (PW)[49] functional in the general gradient approximation and the dispersion-corrected OBS-PW functional (OBS),[50] with the inclusion of hydrogen bonding and vdW interactions. The all-electron method was used to approximate the wave functions with a double numeric and polarization basis sets. The self-consistency threshold of total energy was set at 10^{-6} hartree. In the structural optimization, the tolerance limits for the energy, force, and displacement were set at 10^{-5} hartree, 0.002 hartree/Å, and 0.005 Å, respectively. Harmonic vibrational frequencies were computed by diagonalizing the mass-weighted Hessian matrix.[51]

f2 Figure 2 compares the segment lengths of the O:H−O bond as a function of $(H_2O)_N$ cluster size (N) optimized using the

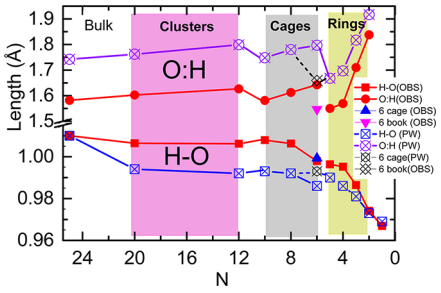

Figure 2. Cluster size dependence of the segmental lengths in the $(H_2O)_N$ clusters. The bond lengths were optimized using the PW[49] and the OBS[50] methods. N = 6 gives the three "cage", "book", and "prism" hexamer structures, all with nearly identical binding energy.[11]

PW and the OBS algorithms. The DFT-derived results are in accordance with those reported in refs 3 and 4. Comparison of results derived from these two DFT methods confirms that: (i) molecular CN reduction shortens the H−O bond and lengthens the O:H and (ii) the shortening (lengthening) of the H−O bond is always coupled to the lengthening (shortening) of the O:H, independent of the algorithm.

As the N is reduced from 24 (an approximation of the number of molecules in bulk water) to two (a dimer), the H−O bond contracts by 4% from 0.101 to 0.097 nm and the O:H bond expands by 17% from 0.158 to 0.185 nm, according to the OBS derivatives. This gives a 13% expansion of O−O distance, which is a significant amount for the dimer. The O:H−O bond angle−length profiles are nonmonotonic because of different effective CNs in different structures. The monotonic O:H and H−O relaxation profiles for $N \leq 6$ will be discussed in the subsequent sections without influencing the generality of conclusions.

Figure 3a shows the N dependence of the $(H_2O)_N$ vibration spectra. As expected, the stiffer ω_H (>2700 cm^{-1}) experiences a blue shift while the softer ω_L undergoes a red shift as the N is reduced. The ω_L shifts from 250 to 180 cm^{-1} as the $(H_2O)_6$ becomes a dimer $(H_2O)_2$. The O:H−O bending mode (400−1000 cm^{-1}) shifts slightly, but the H−O−H bending mode (~1600 cm^{-1}) remains the same. The calculated ω_H blue shift in Figure 3b agrees with that measured in molecular clusters[28,30,42,53,54] and in ice and water surfaces.[27] (See Figures S1 and S2 of the Supporting Information). This consistency validates our predictions regarding the under-coordination-induced asymmetric phonon relaxation dynamics of water molecules.

Figure 4a plots the N dependence of the O−O distance derived from Figure 2. According to our calculations, the O−O distance expands by 8% when the N is reduced from 20 to 3, which is compatible with the value of 5.9% measured in the water surface at 25 °C.[33] The polarization enhancement of the under-coordinated water molecules[4,55] is related to the O−O distance because of the charge conservation of the molecules. As it has been discovered using an ultrafast liquid jet vacuum ultraviolet photoelectron spectroscopy,[56] the dissociation energy for an electron in solution changes from a bulk value of 3.3 to 1.6 eV at the water surface. The dissociation energy, as a proxy of work function and surface polarization, decreases further with molecule cluster size (Figure S3 of the Supporting Information). These findings verify our predictions on the under-coordination-induced volume expansion and polarization of water molecules.

The polarization of molecules caused by both under-coordination and interelectron−pair repulsion enhances the elasticity and the viscosity of the skin of water. The high elasticity and the high density of surface dipoles form the essential conditions for the hydrophobicity of a contacting interface.[57] Therefore, given our established understanding of high elasticity and polarization in under-coordinated water molecules, it is now clear why the monolayer film of water is hydrophobic.[20]

Figure 4b shows the predicted N-dependence of the melting point (T_{mN}) elevation and the O1s core level shift (ΔE_{1sN}). According to eq 2, both T_{mN} and ΔE_{1sN} are proportional to the covalent bond energy in the form of: $T_{mN}/T_{mB} = \Delta E_{1sN}/\Delta E_{1sB} = E_{HN}/E_{HB} = (d_{HN}/d_{HB})^{-4}$. Subscript B denotes the bulk. One can derive from the plots that when the N is reduced from a value of infinitely large to two, the T_{mN} will increase by 12% from 273 to 305 K. It is now clear why the ultrathin water films[7,15−20] or water droplets encapsulated in hydrophobic nanopores[13,14] behave like ice at room temperature. The expected O1s energy shift ($C_z^{-4} - 1$) of water clusters also agrees with the trend of the measurements. (See Figure S4 of the Supporting Information.) For instance, the O1s core level shifts from 538.2 to 538.6 eV and to 539.8 eV when the water cluster size is reduced from N = 200 to 40 and to free water molecules.[26,58]

Thus, a hybridization of the GP H−O bond contraction,[36−38,43] Anderson localization,[39,45] and the segmented hydrogen bond scheme[40,42] has enabled clarification of the observed anomalous behavior of water molecules with fewer than four neighbors such as molecular clusters, hydration shells, and surface skins of liquid water. This exercise also reconciled the anomalies of O−O expansion, O1s electron densification and entrapment, surface electron polarization, high-frequency phonon stiffening, and the ice-like and hydrophobic nature of

dx.doi.org/10.1021/jz401029z | J. Phys. Chem. Lett. XXXX, XXX, XXX−XXX

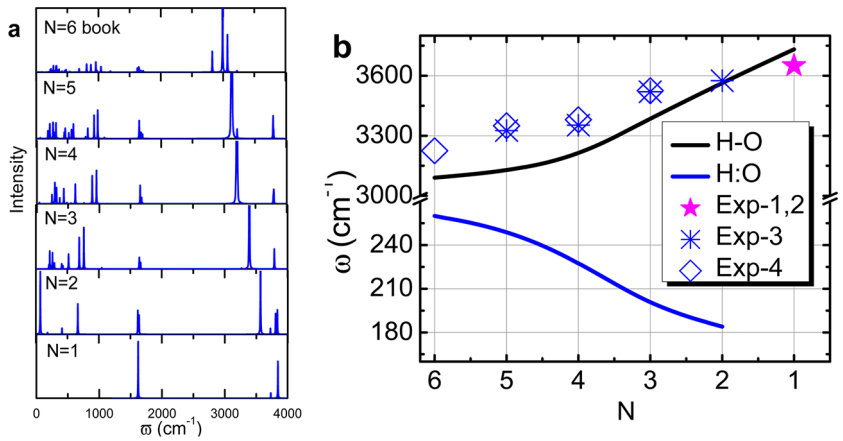

Figure 3. (a) Size dependence of the phonon spectra of $(H_2O)_N$ clusters ($N \leq 6$). (b) Calculated (solid line) ω_H blue shift has a similar trend as the measured frequencies (scattered data) of the H−O phonons of $(H_2O)_N$, shown as Exp-1,[52] Exp-2,[42] Exp-3,[28] and Exp-4.[53] Measurements of the ω_L red shift are not presently available due to experimental limitations.

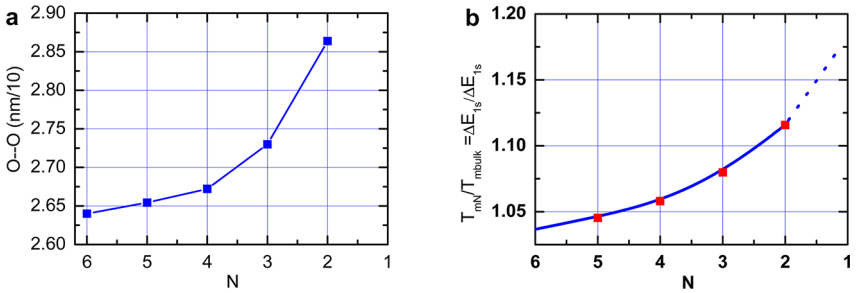

Figure 4. N dependence of (a) the O−O distance, (b) the melting point, T_{mN} (to $N = 2$ for dimers), and the O1s core-level shift (to $N = 1$ for gas monomers) of $(H_2O)_N$ clusters based on DFT-derived d_{HN}/d_{HB} values and eq 2.

such undercoordinated water molecules. Agreement between numerical calculations and experimental observations has verified our hypothesis and predictions:

(i) Under-coordination-induced GP contraction of the H−O bond and interelectron-pair repulsion-driven O:H elongation dictate the unusual behavior of water molecules in the nanoscale O:H−O networks and in the skin of water.

(ii) The shortening of the H−O bond raises the density of the core and bonding electrons in the under-coordinated molecules, which in turn polarizes the nonbonding electron lone pairs on oxygen.

(iii) The stiffening of the H−O bond increases the O1s core-level shift, causes the blue shift of the H−O phonon frequency, and elevates the melting point of water molecular clusters, surface skins, and ultrathin films of water.

(iv) Under-coordinated water molecules could form an ice-like, low-density phase that is hydrophobic, stiffer, and thermally more stable than the bulk water.[5,6]

■ ASSOCIATED CONTENT

Ⓢ Supporting Information

Details of the tetrahedrality of water clusters and methodologies as well as nomenclatures regarding basic concepts published previously but not covered in the main text. This material is available free of charge via the Internet at http://pubs.acs.org.

■ AUTHOR INFORMATION

Corresponding Author

*E-mail: wtzheng@jlu.edu.cn (W.Z.); ecqsun@ntu.edu.sg (C.Q.S.).

Notes

The authors declare no competing financial interest.

■ ACKNOWLEDGMENTS

Special thanks to Philip Ball, Yi Sun, Buddhudu Srinivasa, and John Colligon for their comments and expertise. Financial support from the NSF China (Nos.: 21273191, 1033003, 90922025) is gratefully acknowledged.

■ REFERENCES

(1) Kühne, T. D.; Khaliullin, R. Z. Electronic Signature of the Instantaneous Asymmetry in the First Coordination Shell of Liquid Water. *Nat. Commun.* **2013**, *4*, 1450.

(2) Petkov, V.; Ren, Y.; Suchomel, M. Molecular Arrangement in Water: Random but Not Quite. *J. Phys.: Condens. Matter* **2012**, *24*, 155102.

(3) Keutsch, F. N.; Saykally, R. J. Water Clusters: Untangling the Mysteries of the Liquid, One Molecule at a Time. *Proc. Natl. Acad. Sci.* **2001**, *98*, 10533.

(4) Gregory, J. K.; Clary, D. C.; Liu, K.; Brown, M. G.; Saykally, R. J. The Water Dipole Moment in Water Clusters. *Science* **1997**, *275*, 814.

(5) Liu, K.; Cruzan, J. D.; Saykally, R. J. Water Clusters. *Science* **1996**, *271*, 929.

(6) Ludwig, R. Water: From Clusters to the Bulk. *Angew. Chem., Int. Ed.* **2001**, *40*, 1808.

(7) Michaelides, A.; Morgenstern, K. Ice Nanoclusters at Hydrophobic Metal Surfaces. *Nat. Mater.* **2007**, *6*, 597.

(8) Turi, L.; Sheu, W. S.; Rossky, P. J. Characterization of Excess Electrons in Water-Cluster Anions by Quantum Simulations. *Science* **2005**, *309*, 914.
(9) Verlet, J. R. R.; Bragg, A. E.; Kammrath, A.; Cheshnovsky, O.; Neumark, D. M. Observation of Large Water-Cluster Anions with Surface-Bound Excess Electrons. *Science* **2005**, *307*, 93.
(10) Hammer, N. I.; Shin, J. W.; Headrick, J. M.; Diken, E. G.; Roscioli, J. R.; Weddle, G. H.; Johnson, M. A. How Do Small Water Clusters Bind an Excess Electron? *Science* **2004**, *306*, 675.
(11) Perez, C.; Muckle, M. T.; Zaleski, D. P.; Seifert, N. A.; Temelso, B.; Shields, G. C.; Kisiel, Z.; Pate, B. H. Structures of Cage, Prism, and Book Isomers of Water Hexamer from Broadband Rotational Spectroscopy. *Science* **2012**, *336*, 897.
(12) Ishiyama, T.; Takahashi, H.; Morita, A. Origin of Vibrational Spectroscopic Response at Ice Surface. *J. Phys. Chem. Lett.* **2012**, 3001.
(13) Lakhanpal, M. L.; Puri, B. R. Boiling Point of Capilary-Condensed Water. *Nature* **1953**, *172*, 917.
(14) Li, L.; Kazoe, Y.; Mawatari, K.; Sugii, Y.; Kitamori, T. Viscosity and Wetting Property of Water Confined in Extended Nanospace Simultaneously Measured from Highly-Pressurized Meniscus Motion. *J. Phys. Chem. Lett.* **2012**, 2447.
(15) Xu, K.; Cao, P. G.; Heath, J. R. Graphene Visualizes the First Water Adlayers on Mica at Ambient Conditions. *Science* **2010**, *329*, 1188.
(16) Miranda, P. B.; Xu, L.; Shen, Y. R.; Salmeron, M. Icelike Water Monolayer Adsorbed on Mica at Room Temperature. *Phys. Rev. Lett.* **1998**, *81*, 5876.
(17) McBride, F.; Darling, G. R.; Pussi, K.; Hodgson, A. Tailoring the Structure of Water at a Metal Surface: A Structural Analysis of the Water Bilayer Formed on an Alloy Template. *Phys. Rev. Lett.* **2011**, *106*, 226101.
(18) Hodgson, A.; Haq, S. Water Adsorption and the Wetting of Metal Surfaces. *Surf. Sci. Rep.* **2009**, *64*, 381.
(19) Meng, S.; Wang, E. G.; Gao, S. W. Water Adsorption on Metal Surfaces: A General Picture from Density Functional Theory Studies. *Phys. Rev. B* **2004**, *69*, 195404.
(20) Wang, C.; Lu, H.; Wang, Z.; Xiu, P.; Zhou, B.; Zuo, G.; Wan, R.; Hu, J.; Fang, H. Stable Liquid Water Droplet on a Water Monolayer Formed at Room Temperature on Ionic Model Substrates. *Phys. Rev. Lett.* **2009**, *103*, 137801.
(21) Qiu, H.; Guo, W. Electromelting of Confined Monolayer Ice. *Phys. Rev. Lett.* **2013**, *110*, 195701.
(22) Omar, M. A. *Elementary Solid State Physics: Principles and Applications*; Addison-Wesley: New York, 1993.
(23) Lindemann, F. A. The Calculation of Molecular Natural Frequencies. *Z. Phys* **1910**, *11*, 609.
(24) James, M.; Darwish, T. A.; Ciampi, S.; Sylvester, S. O.; Zhang, Z. M.; Ng, A.; Gooding, J. J.; Hanley, T. L. Nanoscale Condensation of Water on Self-Assembled Monolayers. *Soft Matter* **2011**, *7*, 5309.
(25) Winter, B.; Aziz, E. F.; Hergenhahn, U.; Faubel, M.; Hertel, I. V. Hydrogen Bonds in Liquid Water Studied by Photoelectron Spectroscopy. *J. Chem. Phys.* **2007**, *126*, 124504.
(26) Abu-Samha, M.; Borve, K. J.; Winkler, M.; Harnes, J.; Saethre, L. J.; Lindblad, A.; Bergersen, H.; Ohrwall, G.; Bjorneholm, O.; Svensson, S. The Local Structure of Small Water Clusters: Imprints on the Core-Level Photoelectron Spectrum. *J. Phys. B: At., Mol. Opt. Phys.* **2009**, *42*, 055201.
(27) Kahan, T. F.; Reid, J. P.; Donaldson, D. J. Spectroscopic Probes of the Quasi-Liquid Layer on Ice. *J. Phys. Chem. A* **2007**, *111*, 11006.
(28) Ceponkus, J.; Uvdal, P.; Nelander, B. Water Tetramer, Pentamer, And Hexamer in Inert Matrices. *J. Phys. Chem. A* **2012**, *116*, 4842.
(29) Shen, Y. R.; Ostroverkhov, V. Sum-Frequency Vibrational Spectroscopy on Water Interfaces: Polar Orientation of Water Molecules at Interfaces. *Chem. Rev.* **2006**, *106*, 1140.
(30) Buch, V.; Bauerecker, S.; Devlin, J. P.; Buck, U.; Kazimirski, J. K. Solid Water Clusters in the Size Range of Tens-Thousands of H_2O: a Combined Computational/Spectroscopic Outlook. *Int. Rev. Phys. Chem.* **2004**, *23*, 375.
(31) Abu-Samha, M.; Borve, K. J. Surface Relaxation in Water Clusters: Evidence from Theoretical Analysis of the Oxygen 1s Photoelectron Spectrum. *J. Chem. Phys.* **2008**, *128*, 154710.
(32) Wilson, K. R.; Rude, B. S.; Catalano, T.; Schaller, R. D.; Tobin, J. G.; Co, D. T.; Saykally, R. J. X-ray Spectroscopy of Liquid Water Microjets. *J. Phys. Chem. B* **2001**, *105*, 3346.
(33) Wilson, K. R.; Schaller, R. D.; Co, D. T.; Saykally, R. J.; Rude, B. S.; Catalano, T.; Bozek, J. D. Surface Relaxation in Liquid Water and Methanol Studied by X-Ray Absorption Spectroscopy. *J. Chem. Phys.* **2002**, *117*, 7738.
(34) Lenz, A.; Ojamae, L. a Theoretical Study of Water Equilibria: The Cluster Distribution versus Temperature and Pressure for $(H_2O)(n)$, n=1−60, and Ice. *J. Chem. Phys.* **2009**, *131*, 134302.
(35) Solveyra, E. G.; Llave, E. d. l.; Molinero, V.; Soler-Illia, G. J. A. A.; Scherlis, D. A. Structure, Dynamics, and Phase Behavior of Water in TiO_2 Nanopores. *J. Phys. Chem. C* **2013**, *117*, 3330.
(36) Pauling, L. Atomic Radii and Interatomic Distances in Metals. *J. Am. Chem. Soc.* **1947**, *69*, 542.
(37) Goldschmidt, V. M. Crystal Structure and Chemical Correlation. *Ber Deut Chem Ges* **1927**, *60*, 1263.
(38) Feibelman, P. J. Relaxation of hcp(0001) Surfaces: A Chemical View. *Phys Rev B* **1996**, *53*, 13740.
(39) Abrahams, E.; Anderson, P. W.; Licciardello, D. C.; Ramakrishnan, T. V. Scaling Theory of Localization: Absence of Quantum Diffusion in Two Dimensions. *Phys. Rev. Lett.* **1979**, *42*, 673.
(40) Sun, C. Q.; Zhang, X.; Zheng, W. T. Hidden Force Opposing Ice Compression. *Chem. Sci.* **2012**, *3*, 1455.
(41) Vacha, R.; Marsalek, O.; Willard, A. P.; Bonthuis, D. J.; Netz, R. R.; Jungwirth, P. Charge Transfer between Water Molecules As the Possible Origin of the Observed Charging at the Surface of Pure Water. *J. Phys. Chem. Lett.* **2012**, *3*, 107.
(42) Sun, Q. The Raman OH Stretching Bands of Liquid Water. *Vib. Spectrosc* **2009**, *51*, 213.
(43) Sun, C. Q. Size Dependence of Nanostructures: Impact of Bond Order Deficiency. *Prog. Solid State Chem.* **2007**, *35*, 1.
(44) Zhao, M.; Zheng, W. T.; Li, J. C.; Wen, Z.; Gu, M. X.; Sun, C. Q. Atomistic Origin, Temperature Dependence, And Responsibilities of Surface Energetics: An Extended Broken-Bond Rule. *Phys. Rev. B* **2007**, *75*, 085427.
(45) Sun, C. Q. Dominance of Broken Bonds and Nonbonding Electrons at the Nanoscale. *Nanoscale* **2010**, *2*, 1930.
(46) Sun, C. Q. Surface and Nanosolid Core-Level Shift: Impact of Atomic Coordination-Number Imperfection. *Phys. Rev. B* **2004**, *69*, 045105.
(47) Sun, C. Q.; Pan, L. K.; Li, C. M.; Li, S. Size-Induced Acoustic Hardening and Optic Softening of Phonons in InP, CeO_2, SnO_2, CdS, Ag, and Si Nanostructures. *Phys Rev B* **2005**, *72*, 134301.
(48) Sun, C. Q.; Shi, Y.; Li, C. M.; Li, S.; Yeung, T. C. A. Size-Induced Undercooling and Overheating in Phase Transitions in Bare and Embedded Clusters. *Phys. Rev. B* **2006**, *73*, 075408.
(49) Perdew, J. P.; Wang, Y. Accurate and Simple Analytic Representation of the Electron-Gas Correlation-Energy. *Phys. Rev. B* **1992**, *45*, 13244.
(50) Ortmann, F.; Bechstedt, F.; Schmidt, W. G. Semiempirical Van Der Waals Correction to the Density Functional Description of Solids and Molecular Structures. *Phys. Rev. B* **2006**, *73*, 205101.
(51) Wilson, E. B.; Decius, J. C.; Cross, P. C. *Molecular Vibrations*; Dover: New York, 1980.
(52) Cross, P. C.; Burnham, J.; Leighton, P. A. The Raman Spectrum and the Structure of Water. *J. Am. Chem. Soc.* **1937**, *59*, 1134.
(53) Hirabayashi, S.; Yamada, K. M. T. Infrared Spectra and Structure of Water Clusters Trapped in Argon and Krypton Matrices. *J. Mol. Struct.* **2006**, *795*, 78.
(54) Pradzynski, C. C.; Forck, R. M.; Zeuch, T.; Slavicek, P.; Buck, U. a Fully Size-Resolved Perspective on the Crystallization of Water Clusters. *Science* **2012**, *337*, 1529.
(55) Yang, F.; Wang, X.; Yang, M.; Krishtal, A.; van Alsenoy, C.; Delarue, P.; Senet, P. Effect of Hydrogen Bonds on Polarizability of a

468 Water Molecule in $(H_2O)(N)$ (N = 6, 10, 20) Isomers. *Phys. Chem.*
469 *Chem. Phys.* **2010**, *12*, 9239.
470 (56) Siefermann, K. R.; Liu, Y.; Lugovoy, E.; Link, O.; Faubel, M.;
471 Buck, U.; Winter, B.; Abel, B. Binding Energies, Lifetimes and
472 Implications of Bulk and Interface Solvated Electrons in Water. *Nat*
473 *Chem* **2010**, *2*, 274.
474 (57) Li, J.; Li, Y. X.; Yu, X.; Ye, W. J.; Sun, C. Q. Local Bond Average
475 for the Thermally Driven Elastic Softening of Solid Specimens. *J. Phys.*
476 *D: Appl. Phys.* **2009**, *42*, 045406.
477 (58) Bjorneholm, O.; Federmann, F.; Kakar, S.; Moller, T. Between
478 Vapor and Ice: Free Water Clusters Studied by Core Level
479 Spectroscopy. *J. Chem. Phys.* **1999**, *111*, 546.